Results of the South African Cloud-Seeding Experiments Using Hygroscopic Flares

G. K. MATHER

CloudQuest, Nelspruit, South Africa

D. E. TERBLANCHE

Weather Bureau, Bethlehem, South Africa

F. E. STEFFENS AND L. FLETCHER

Unisa, Pretoria, South Africa

(Manuscript received 29 April 1996, in final form 21 February 1997)

ABSTRACT

A new method of seeding convective clouds for the purpose of augmenting rainfall is being developed in South Africa. Flares that produce small salt particles (0.5-μm mean diameter) are attached to the trailing edge of the wings of seeding aircraft and ignited in updrafts below the cloud base of convective storms. This method of delivery overcomes most of the difficulties encountered in the handling and the use of hygroscopic materials, difficulties that made seeding with ice nuclei (AgI) a more attractive option.

The research that has led to the development of this new technique was prompted by an encounter with a storm with dramatically altered microphysics that was growing over a Kraft paper mill in the research area. Hygroscopic seeding flares were subsequently developed, and seeding trials began in October 1990. Successful seeding trials quickly led to the design and execution of a randomized convective cloud-seeding experiment, the results of which show convincing evidence of increases in the radar-measured rain mass from seeded storms when compared to the control or unseeded storms.

Heightened reflectivities aloft seen by the real-time storm-tracking software and observed in the exploratory analysis raises the possibility of developing a radar-measured seeding algorithm that can recognize in almost real time a successful convective seeding event. The implications of such a development would have far-reaching effects on the conduct of future convective cloud-seeding experiments and operations.

The authors' seeding hypothesis postulates that the hygroscopic seeding at cloud base accelerates the growth of large hydrometeors in the treated clouds, which harvest more of the available supercooled water before it is expelled into the anvils by the strong updrafts that are a characteristic of the local storms, thereby increasing the *efficiency* of the rainfall process. The validity of this hypothesis is supported by microphysical measurements made from an instrumented Learjet and the results of the randomized experiment, both of which are supported by numerical condensation–coalescence calculations. There are also indications that the hygroscopic seeding may have an impact upon the dynamics of the treated storms, lengthening their lifetimes by strengthening the coupling of the updraft–downdraft storm propagation mechanism.

The apparent sensitivity of rainfall in convective clouds to the aerosol concentration, size, and chemical content may have climatic implications. Higher concentrations of small aerosols produced by pollution, biomass burning, etc., could adversely affect the efficiency of the rainfall process. The negative consequences of this effect would be magnified in regions that depend upon convective storms to provide the bulk of their annual rainfall.

1. Introduction

The search for a method of augmenting rainfall from convective storms, which provide the bulk of the rain to the summer rainfall regions of South Africa, has been pursued for over 15 years.

For the past several years, the research in two areas (Nelspruit in the Eastern Transvaal and Bethlehem in the Free State) has been focused on rainfall efficiency. The thunderstorms that have been studied in these areas are generally not efficient producers of rainfall. Much of the moisture ingested by these storms is lofted by strong updrafts into the huge anvil clouds that are a common feature in the summer skies of the study areas. The challenge, then, has been to find a way to produce large particles early in the limited lifetimes of the cells, which form the units of the multicellular storms common to the region. The hope is that these larger particles will harvest more of the available cloud water before it

Corresponding author address: Dr. Graeme K. Mather, CloudQuest, P.O. Box 1135, Nelspruit 1200, South Africa.
E-mail: mather@soft.co.ZA

is lost to the anvil, thereby increasing the *efficiency* of the rainfall process.

Our initial approach to rainfall augmentation efforts was to use the well-known glaciogenic seeding materials, silver iodide and dry ice, delivered into growing convective cells at around the −10°C isotherm. The advent of the laser probes meant that the ice crystal production capabilities of the two materials could be assessed in seeding trials. The trials at Nelspruit indicated that dry ice was producing ice crystals earlier and in greater concentrations than silver iodide (Garstang et al. 1981). These and the results from the HIPLEX tests (Dennis et al. 1984) led to the choice of dry ice as the seeding agent for the first Nelspruit randomized seeding experiment. This exploratory experiment, conducted over 3 years, indicated a response from a category of clouds in which coalescence was probably playing a role in the rainfall formation processes. There was an almost fourfold percentage increase in radar-measured rain flux and storm area when the seeded and control storms were compared. The experiment was exploratory because we were not sure at that stage what sort of seeding response to expect from multicellular storms (Mather et al. 1996). This previous work and the current paper should be read in sequence, since the results reported here are a logical outcome of work with dry ice. The seeding hypothesis that emerged from the dry ice seeding experiment is discussed in the conclusions section of this paper.

On an extension of this experiment, dramatically enhanced coalescence was unexpectedly observed by our cloud physics Learjet while penetrating clouds that were developing on the flanks of a large thunderstorm. Huge drops (diameters 4–6 mm) were encountered in strong (10–15 m s^{-1}) updrafts at around the −10°C level. What was novel about these measurements was that, according to our extensive cloud physics database, drops of this size should not have occurred in a storm growing in that thermodynamic environment. Recirculation of particles from a downdraft into an updraft on the edge of the storm could be a possible explanation for these observations, but if so, this would be the first such observation in our microphysical database. Analysis of the radar data showed that the storm was growing almost directly over a Kraft paper mill that had recently undergone a fourfold expansion. Subsequent sampling of cumulus clouds in the vicinity of the paper mill showed broadening of cloud drop spectra similar to that reported by Eagan et al. (1974). It was the broadening of the droplet spectra at cloud base by hygroscopic particles emitted by the mill that presumably resulted in the enhanced coalescence observed by the Learjet (Mather 1991).

These observations suggested the possibility of using a pyrotechnic flare to produce similar sizes of particles of less noxious materials for experimental purposes. Although we could not hope to equal the mill output, we reasoned that if the material was placed at exactly the right place at the right time, similar effects might be achieved in treated storms. A flare, based on a formulation developed at the Naval Weapons Center at China Lake for producing fog (Hindman 1978), was designed and manufactured locally.

While hygroscopic seeding is not new, most experiments to date have used finely ground salt particles, usually larger than about 10 μm. The disadvantages of this approach are the weight that has to be carried for any practical applications and the difficulty in handling and dispensing the highly hygroscopic and corrosive salt particles. Also, the growth rates of the salt embryos to raindrops must be matched well to the updraft profile, or their growth will be inefficient (Klazura and Todd 1978). While some positive effects have been attributed to such seeding (Biswas and Dennis 1971), the logistics of handling the hygroscopic salts have made this method less attractive than ice nuclei seeding.

The approach reported here uses easily handled pyrotechnic flares that produce small salt particles, average size around 0.5 μm, that broaden the cloud base droplet spectra thus accelerating coalescence. Our hypothesis is that this increases the efficiency of the rain formation process in treated storms. The operational advantages of this method are the amount of salt required is much less, the salt particles are readily produced by flares, the target area for seeding is an easily identified region at cloud base where the initial droplet spectrum is determined, dispersion of the material is much easier, and long-term storage of the flares presents no problems.

A three-pronged approach has been adopted in evaluating the efficacy of these new cloud-seeding flares. First was the search for microphysical changes in seeded clouds using our instrumented Learjet, reported in section 2 of this paper. The presence of a large and clear response at aircraft sampling scales was considered a necessary precursor to any randomized seeding experiment, since, if changes were not detected here, it is unlikely that changes would be detected at the radar sampling scales that would be used to judge the outcome of an experiment. Second was a 5-yr randomized cloud-seeding experiment, the results of which are presented in section 3. Finally, numerical condensation–coalescence calculations were performed using as input observations collected near Nelspruit. The results from this study strongly support both the microphysical measurements and the statistical results from the randomized experiment (Cooper et al. 1997).

2. Measurements—Microphysical responses and flare characteristics

The path followed in evaluating this new cloud-seeding device was to first determine whether the flares were capable of producing the desired changes in cloud microphysics. Success in this first stage (defined here as detecting changes in the microphysical properties of seeded clouds commensurate with the hygroscopic seeding hypothesis) was followed by analyses of the chem-

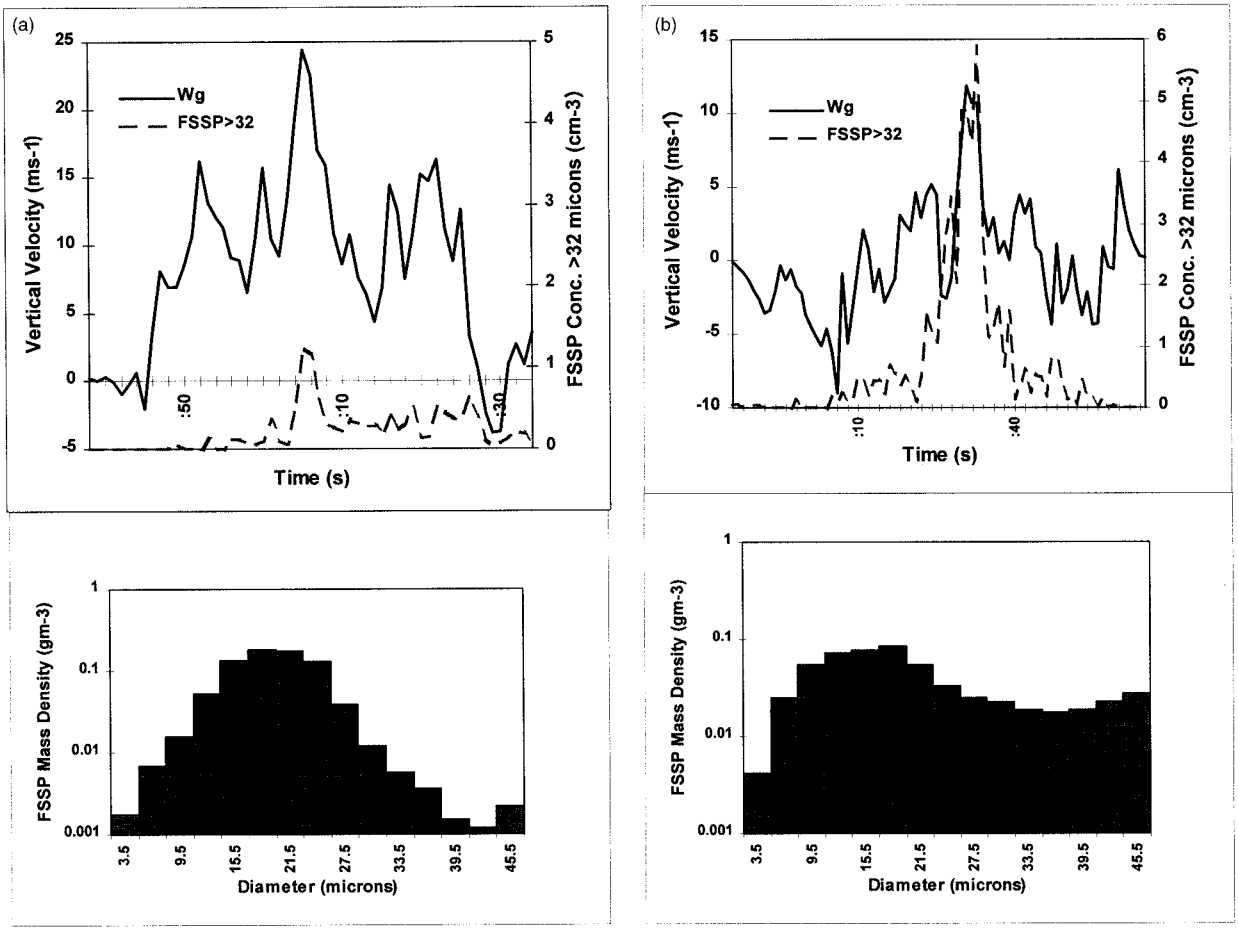

FIG. 1. FSSP droplet concentrations greater than 32 μm and vertical velocities measured on two passes through a cloud seeded with hygroscopic flares on 9 October 1990. The histograms show the distribution of cloud water (gm^{-3}) between 2 and 47 μm averaged over 1 km centered around the maximum updraft speeds: (a) 2 min after seeding commenced at cloud base and (b) 6 min after seeding commenced (see text for further details).

ical content of the combustion products and measurements of the dry particle spectrum.

a. Seeding trials

Initially, a batch of 20 500-g flares were manufactured for use in exploratory seeding trials. First, experiments were conducted using the flare-equipped seeding aircraft at cloud base, the project radar in volume or sector scan mode, and the project's Learjet sampling at around the -10°C level. The objective of these first trials was to test the seeding hypothesis—that is, that the release of small hygroscopic particles into the updraft at cloud base would accelerate or enhance the formation of precipitation via coalescence in treated clouds. Clouds tested in these experiments had cloud base temperatures between 5° and 15°C and were multicell thunderstorms. The updrafts were located around the western flank of the storms, often close to, but always clear of the rain shaft. Strength of the updraft varied and appeared to be a function of storm size. No quantitative updraft measurements were made by the seeding aircraft, as this would have required straight and level flight, a pattern not possible with the requirement of keeping the aircraft close to the updraft core.

The second trial, reported here in some detail, took place on 9 October 1990. Two flares were ignited by the seeding aircraft at 1556 LT (all times quoted here are South African local times—UTC + 2 h) in the updraft beneath a small storm. Cloud base temperature was 11.4°C. An additional two flares were ignited at 1600 LT. The Learjet had commenced sampling the cloud turrets rising on the flank of the storm at 1554 LT at around the -10°C level (about 5900 m above mean sea level). Mean updraft speeds were between 8 and 9 m s^{-1}. The Learjet first encountered evidence of seeding effects at 1602 LT. Since the seeding aircraft was operating at a height of around 3000 m, the seeding material would have to rise at a rate of around 8 m s^{-1} to reach the altitude of the Learjet in the available 6 min, which is close to the observed updraft speeds. Figures 1a and 1b display time histories of droplet concentra-

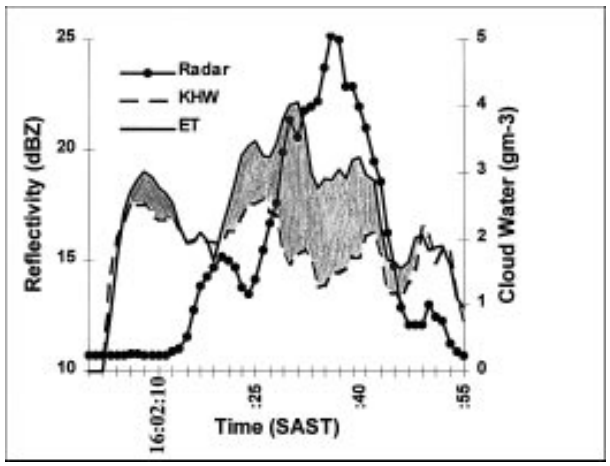

FIG. 2. King hot wire measurement of cloud water, ET measurement of total cloud water, and equivalent reflectivity returns from the aircraft radar measured on the pass shown in Fig. 1b.

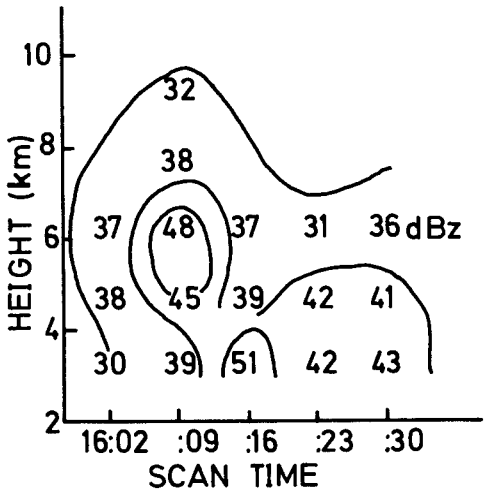

FIG. 3. Time–height plot of peak reflectivities record by Carolina radar in the storm seeded on 9 October 1990. Seeding commenced at 1556 LT.

tions greater than 32 μm and spectra measured by the Particle Measurement Systems (PMS) forward-scattering spectrometer probe (FSSP) as well as updraft profiles measured on passes 2 and 3 through the seeded storm. The histograms show the distribution of cloud water mass between 2 and 47 μm averaged over 1 km centered around the maximum updraft speeds. On pass 2, which commenced at 1558 LT, the recorded distribution of cloud water was typical of clouds sampled in the research areas. On the third pass (1602 LT), a peak in FSSP concentrations greater than 32 μm was observed as well as a flattened distribution of cloud water mass around the maximum updraft speed. Drops toward the 47-μm end of the FSSP spectrum are large enough to continue to grow via coalescence. Distributions of cloud water mass of this shape are not found in updraft regions at these levels in local clouds.

A comparison of the engine temperature (ET) measurement of total condensed water, the PMS–King hot wire (KHW) measurement of cloud water, and returns from the X-band aircraft radar for pass 3 is shown in Fig. 2. Briefly, the measurement of total cloud water is obtained by monitoring the temperature of the air tapped off the eight-stage of the jet engine compressor. Since all condensed water in the cloud (cloud water plus precipitation) has been vaporized by the time the measurement takes place, the mixing ratio m, can be estimated from

$$m = c_p dT/L, \tag{1}$$

where m is the mass of water vapor per unit mass of dry air, c_p is the specific heat of dry air at constant pressure, L is the latent heat of vaporization, and dT is the change in temperature. The KHW measures cloud water in droplets whose diameters are less than about 100 μm. The signal from the X-band radar is obtained by locking the radar facing forward and sampling a single range gate 1500 m ahead of the aircraft. This signal is suitably lagged so that the radar and other measurements coincide. Note that the measurements of cloud water by the ET and the KHW agree at the beginning and end of the penetration, where the radar signal is less than 12 dBZ. In the center of the run, the ET measurement of total condensed water exceeds the KHW measurement of cloud water, indicating that about half the available cloud water has been converted into precipitation (drops exceeding 100 μm in diameter). This interpretation is supported by the radar signal, which reaches about 26 dBZ in this region. Unfortunately, problems with the 2D-C probe on this flight prevented acquisition of any large drop images that might have been present.

Figure 3 shows a time versus height record of maximum reflectivities recorded by the project radar operating in volume scan mode. A pocket of high reflectivity (48 dBZ) occurred aloft about 13 min after seeding commenced, and the maximum reflectivity was observed close to cloud base 7 min later. This storm was not raining when the flares were first ignited.

Many instances have been recorded of large drops appearing at Learjet sampling levels shortly after seeding begins at cloud base, only two of which will be presented here. It is possible that some of the drops may have been caused by ingestion of embryos from the parent cloud. However, the sampling by the Learjet began before the seeding commenced in fresh cloud turrets that were rising on the flanks of the test clouds. Drop images were not present prior to the commencement of seeding at cloud base. The timing of the appearance of the large drops was also carefully observed and occurred with regularity some 6–10 min after seeding began in the updraft at cloud base. Also, the size of some of the drops exceeded anything experienced previously in unseeded clouds. Finally, the radar profiles were often altered shortly after the seeding began, showing high re-

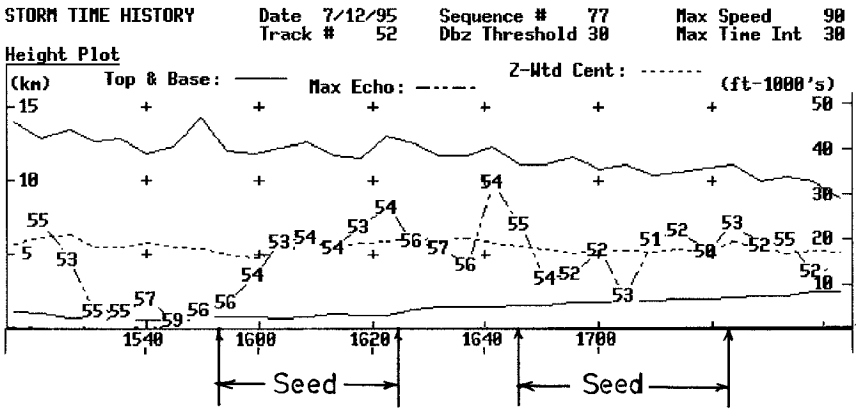

FIG. 4. Time history of a storm seeded with hygroscopic flares showing the heights of the maximum reflectivities recorded before and after seeding commenced. Also shown in this figure are the radar-measured cloud-top heights and bases and the reflectivity-weighted centroids (storm center of gravity). The normal maximum reflectivity vs height pattern is a saw-tooth pattern in which the maximum reflectivity remains above the centroids for one or two scans before descending to cloud base.

flectivities at high levels in the treated cloud. This, in our view, constitutes a radar seeding signal that is completely congruent with the microphysical measurements. Figure 4 depicts a time–height plot of maximum reflectivities with seeding times shown. Typically, the maximum reflectivities show a sawtooth pattern, with the maximum reflectivities staying aloft for one or two scans, then descending to cloud base. Here, we see the maximum reflectivities staying aloft for six consecutive scans after the first seeding run.

On 8 April 1993, large drops were recorded by a PMS 2D-C laser probe in a 10–15 m s^{-1} updraft at a temperature of around -13°C. The measurement of total condensed water by a Lyman-alpha (LA) technique (Morgan et al. 1989), the KHW measurement of cloud water, and the signal from the aircraft's radar are depicted in Fig. 5. Here, the radar signal reached 45 dB*Z*, commensurate with the large drops shown in the figure, two of which exceeded 5 mm in diameter. Again, about half the cloud water has been converted into precipitation. (Note the agreement between the LA and KHW measurement of cloud water at the end of the run where the signal from the radar is around 5 dB*Z*.)

The appearance of such large drops in seeded storms at sampling altitudes prompted replacing the PMS 2D-C (35 to 1120+ μm) with a 2D-P laser probe (range 200 μm to 6+ mm). Figure 6 shows the temperature, updraft, and liquid water recorded in a seeded cloud on 29 March 1994. The large drops imaged by the 2D-P probe on this pass, some of which exceed 6 mm in diameter, occured in an updraft of around 15 m s^{-1}. Clearly, coalescence was well advanced in this cloud.

b. Flare measurements

The success of the initial seeding trials led to the next step, which was to measure the chemical contents and to determine the shape of the dry particle spectrum of the combustion products released by the flares. A sample flare was sent to laboratories in Johannesburg where the mixture was burned in a wind tunnel and the residue, collected on filters, was analyzed by x-ray diffraction and scanning electron microscopy techniques. The flare composition is 18% hydrocarbon binder, 5% magnesium, 10% sodium chloride, 65% potassium perchlorate, and 2% lithium carbonate. The combustion products proportions, similar to those deduced by Hindman (1978), are listed in Table 1. The size of most of the material was estimated at between 0.2 and 0.6 μm. Less than 5% of the particles had diameters between 100 and 180 μm.

The next series of measurements were made in dry air by an instrumented aircraft flying in trail about 50 m behind the seeding aircraft. Since the flare emits a broad particle spectrum, two PMS laser probes covering a range between 0.1 to 47 μm were used for these measurements: a passive cavity aerosol spectrometer probe (PCASP-100X) and an FSSP-100. Most of these measurement were made from the Weather Bureau Aero Commander 690, since the probes on this aircraft are mounted on the nose, making it easier to keep the instruments in the plume from the flare. One surprise was the images recorded by the 2D-C probe, which was mounted next to the other probes. Particles with diameters between 100 and 300 μm were encountered in concentrations of about eight per liter.

The dry particle distributions measured by the PCASP-100X and the FSSP-100 probes are combined in Fig. 7, which shows a long tail toward the large particle end of the spectrum. Curiosity about the nature of the particles larger than 100 μm detected by the 2D-C imaging probe led to efforts to collect these particles for laboratory analyses. Sticky glass slides were held in the plume of a burning flare while the seeding aircraft

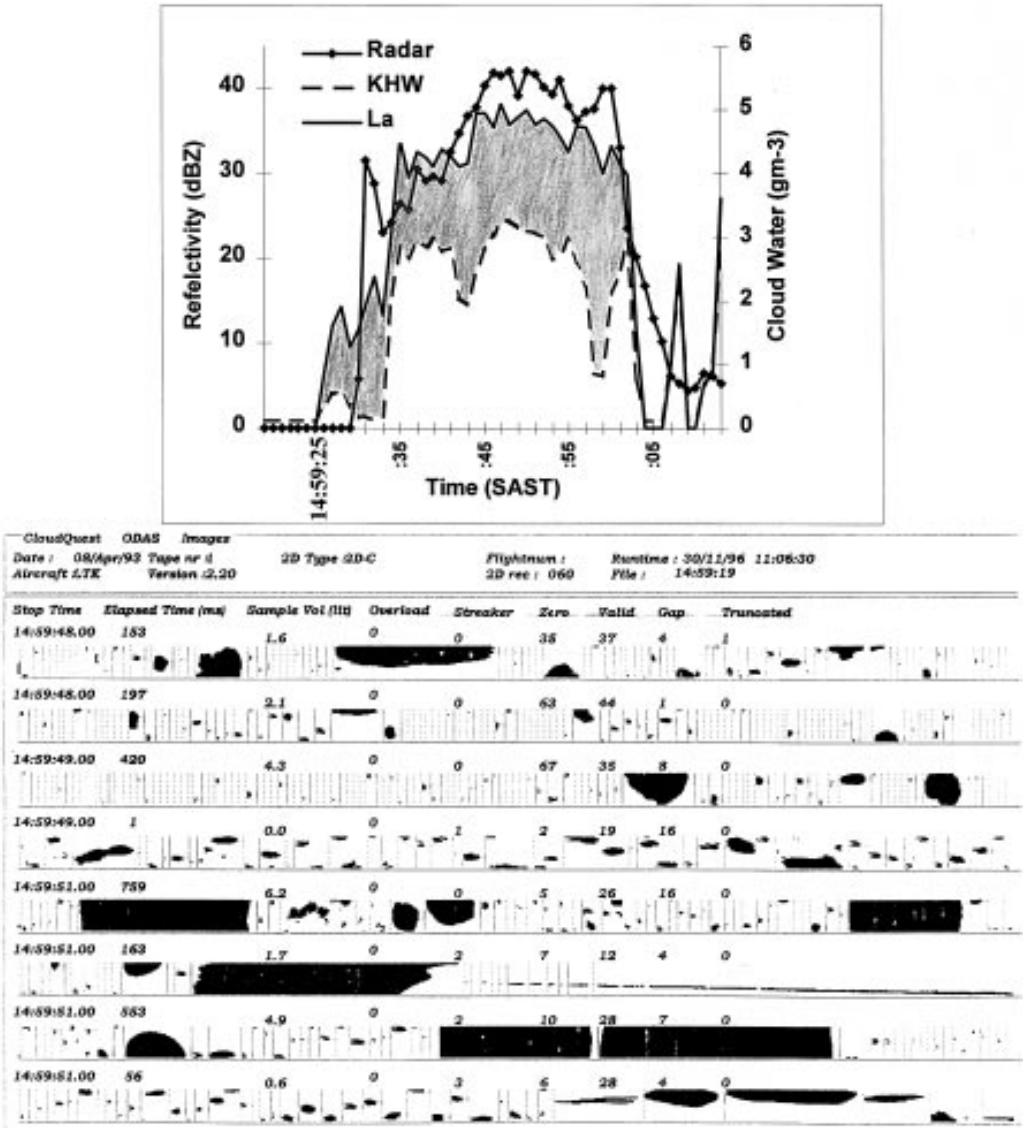

FIG. 5. Lyman-alpha and King hot wire measurements of cloud water and the return from the aircraft's radar from a cloud sampled on 8 April 1993 and images captured by a 2D-C probe through the same cloud. These images were acquired between 1459:48 and 1459:51 LT and coincide with the maximum recorded radar reflectivity. The vertical lines separating the images are 1.12 mm long.

was stationary on the ground, engines running. Several of these slides were sent to a laboratory at the University of the Witwatersrand for x-ray diffraction and scanning electron microscopy analyses. Figure 8 is an electron microscope photograph of one of the larger particles captured on the slides. The x-ray diffraction analysis of this particle identified the elements potassium and chlorine. At this stage of our work, the relative importance of the larger versus the smaller particles in accelerating coalescence is not known.

The initial results from the hygroscopic seeding experiment (section 3), supported by the microphysical changes measured in seeded clouds, caught the attention of scientists from NCAR. Two of these scientists journeyed to Nelspruit in November 1992 to participate in an intensive 3-week measurement program. The portion of the dry particle spectrum between 0.1 and 3 μm was determined during this period, but perhaps the most important measurement was made in the seeded plume about 200 m above cloud base. This was accomplished by flying the Learjet carrying an FSSP-100 probe (size range 2–47 μm) in trail behind the seeding aircraft under the cloud base of an active storm. On encountering a good updraft, the seeding aircraft ignited two flares. The plume from the flares was clearly visible and the Learjet attempted to follow the plume as it rose into the base of the cloud. This is a crucial measurement, since cloud droplet spectra are determined in the first 100 to 200 m

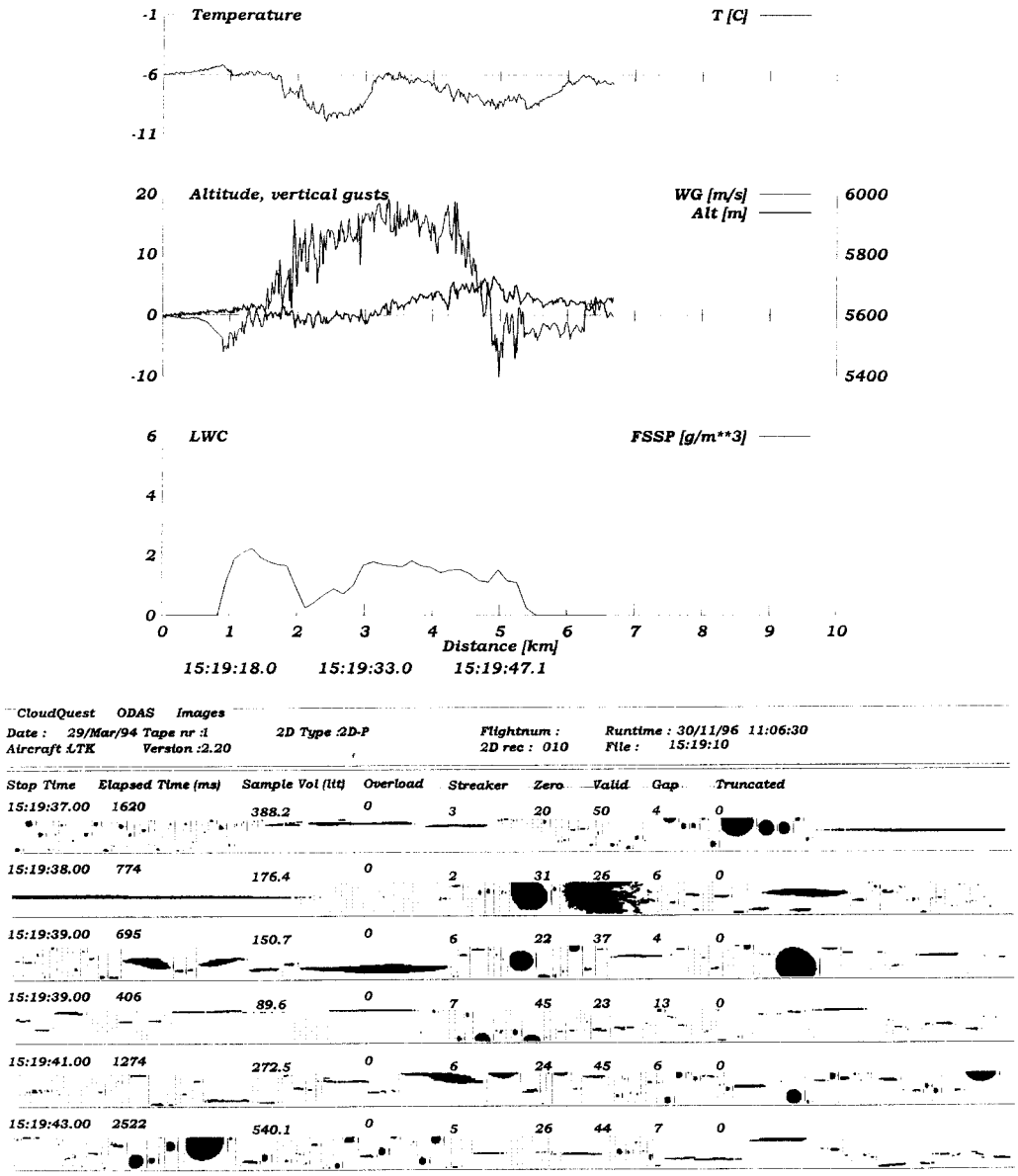

FIG. 6. Time histories through a cloud turret on the flank of a storm sampled near Nelspruit, showing static temperature, true gust velocity, altitude, and liquid water content measured by an FSSP-100 as well as images of particles collected by a 2D-P laser probe. The drops shown here were collected toward the end of the 15 m s^{-1} updraft shown in the figure and at a temperature of −6°C. The vertical lines separating the images here are 6.4 mm long.

Table 1. Combustion products of the hygroscopic seeding flares determined by laboratory tests and deduced by Hindman (1978).

Material	Hindman (%)	Laboratory (%)
Sodium chloride (NaCl)	19	21
Potassium chloride (KCl)	65	67
Lithium carbonate ($LiCO_3$)	1	—
Magnesium oxide (MgO)	15	12

above cloud base, and it is the shape of these spectra that determine the future evolution of rainfall formation in clouds. The measurements (Fig. 9) showed that the material from the flares had dramatically altered the droplet spectrum, presumably by lowering the peak supersaturations reached in the lower layers of the cloud. This reduced the number of natural cloud condensation nuclei (CCN) that was activated, resulting in condensation on fewer, but larger droplets. Note that the liquid water contents of both measurements are about equal, indicating that the measurements were made in the same

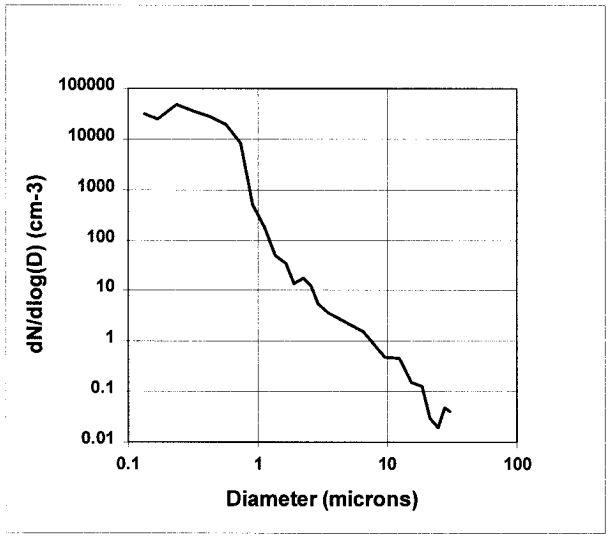

FIG. 7. Dry particle spectrum of combustion products from the hygroscopic seeding flare measured by an instrumented aircraft flying 50 m in trail behind the seeding aircraft using a PCASP-100X and an FSSP-100 probe.

air parcel. These altered spectra are believed to lead to accelerated precipitation growth in treated clouds.

3. The randomized hygroscopic cloud-seeding experiment

A season of successful seeding trials led to the design and execution of a randomized cloud-seeding experiment using the new flares. The anticipated response variable, specified before the experiment commenced, was radar-measured rain mass at base scan using $Z = 200 R^{1.6}$ (Marshall and Palmer 1948). An experiment designed to test the seeding hypothesis began at the beginning of the 1991–92 season (first experiment, 15 October), using the following equipment. The Weather Bureau Aero Commander 690 and the Water Research Commission (WRC) Commander 500S were equipped with seeding racks attached to the rear of the engine nacelles. Each seeding rack held 10 1-kg flares, which were electrically ignited from a firing panel in the cockpit. The WRC cloud physics Learjet was used to make microphysical measurements at around the −10°C level in both natural and seeded clouds. The experiments were conducted within about a 100-km radius of the two C-band radars located at Bethlehem in the Free State and Carolina (near Nelspruit) in the Eastern Transvaal (see Fig. 10). Both radars were operated in volume scan mode, collecting a complete scan about once every 5 min.

a. Experimental design

The experiment was designed in conjunction with the Centre of Applied Statistics at the University of South Africa (Unisa). Two sets of paired envelopes were prepared at Unisa, one for the Bethlehem experiments, the second for Nelspruit. One set of each of the pairs was held at the Carolina and Bethlehem radars. Matching pairs were held in the two seeding aircraft. Launching criterion was the appearance on radar of two or more separate echoes exceeding 40 dB*Z*. After take off, the seeding and the cloud physics aircraft were directed to the storm of interest (usually the strongest echo). On finding a suitable updraft, the pilot of the seeding aircraft would confirm with the radar operator that both the selected storm and his transponder return were clearly visible on radar. All storms selected for an experiment were producing a radar echo before seeding began and most of them were already raining. Criteria for selection were deliberately broad since we did not know what storms (if any) would respond to treatment. For the first three seasons of the experiment, very large storms and squall lines were excluded. The absence of the cloud physics aircraft did not preclude an experiment. With the above conditions fulfilled, the pilot of the seeding aircraft would declare a case (decision time), at which time the radar operator would open the appropriate envelope and broadcast the decision to the seeding pilot who would open his matching envelope. The possible combinations and outcomes are listed in Table 2.

Since the seeding pilot did not reveal the contents of his envelope, both the radar operator and the cloud physics aircraft crew were ''blind'' as to treatment, eliminating any possible biases in the collection of the radar and the cloud physics data. Whatever the outcome, the seeding aircraft stayed with the selected storm for a minimum of 15 min after decision time. For the first three seasons, a maximum of 10 flares were used per experiment, so a second experiment could be selected before the seeding aircraft returned to base. A second storm had to be at least 20-km distance from the first selection. For the last two seasons of the 5-yr experiment, no limit was placed upon the number of flares used per storm up to the maximum of 20 carried on each aircraft.

b. Results—Formal analysis

This first analysis uses the radar-measured rain masses from all 127 storms (62 seeded and 65 controls) from the 5-yr experimental period. Recall that this response variable was specified before the experiment commenced. The tracking software traces the storm including the treated cloud turrets, on the assumption that later ingestion of these turrets will alter the characteristics of the storm. Thus, pretreatment rainfall is calculated for the whole cloud mass. No attempt is made at tracking the individual treated turrets. Storms collected by both radars were analyzed using the objective storm-tracking algorithm developed by Dixon and Mather (1986). Briefly, in each scan, the software identifies the storms, a storm being defined as a contiguous volume all of which

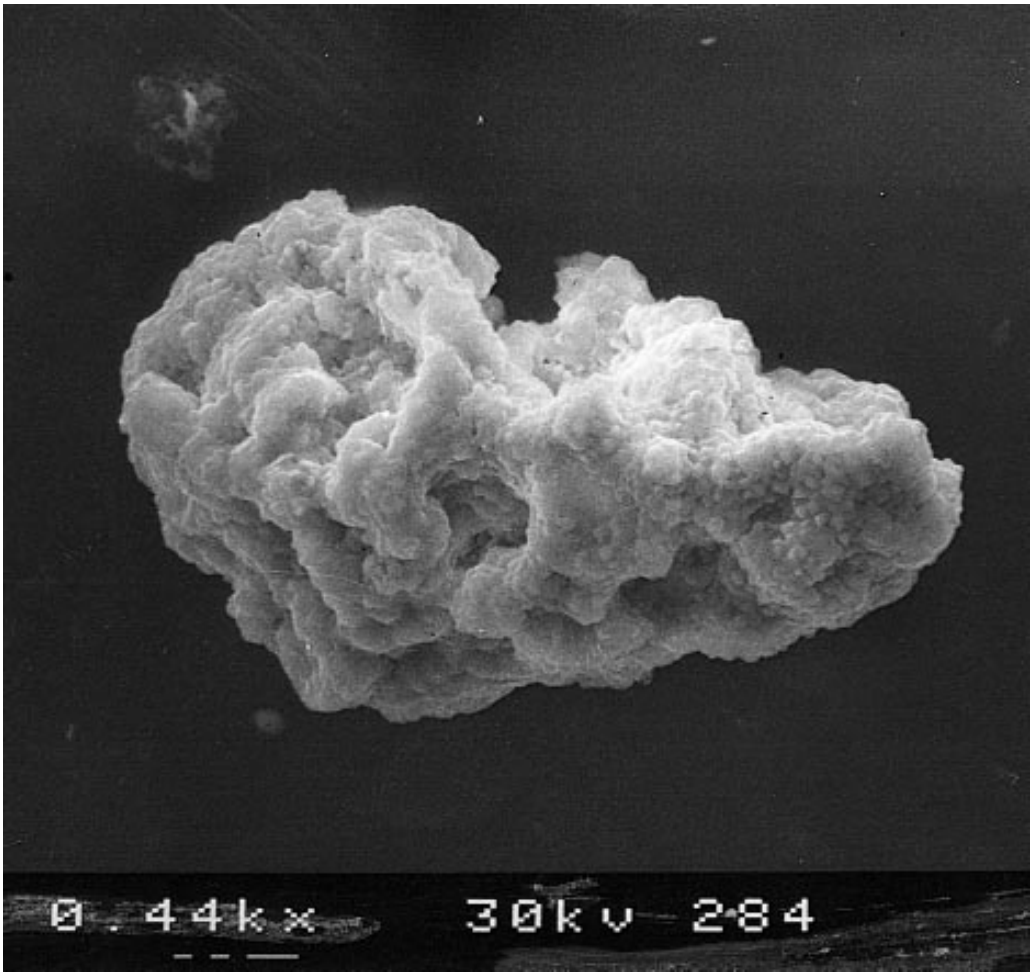

FIG. 8. Electron microscope photograph of a large particle collected on a sticky slide held in the plume of a flare burning on the seeding aircraft on the ground with engines running. Horizontal dimension of this particle is about 165 μm.

exhibits equivalent reflectivities equal to or exceeding 30 dB*Z*. The storm-tracking scheme then joins together the storms from each scan based upon distances between centroids, speeds and directions of movement, relative changes in volume, etc. The statistical analyses are conducted on properties derived from the storm tracks, such as storm durations, volumes, echo heights, and rain masses. A list of all 127 storm track properties that are computed by the software can be found in Mather et al. (1996). The experiments were identified by coincidence in space and in time of the seeding aircraft and storm tracks.

The technique that has provided the most useful insight into revealing differences between the seeded and control storms has been the analysis of these differences in 10-min time windows on either side of decision time. The advantages of this approach are that an assessment of any inadvertent selection biases can be gained by looking at storm track properties in the 10-min interval before decision time, and the validity of any differences between the seeded and untreated storms can be checked for physical consistency as they evolve from one time window to the next. For example, it would be unreasonable to attribute to seeding differences in rain flux found at cloud base in the first 10 min after decision time.

Lifting the limit on storm size for the last two seasons led to the selection of a few very large storms. Calculations of mean storm rain masses were dominated by these few outliers, not an uncommon problem encountered in convective cloud-seeding experiments. We circumvented this problem by dividing the data into quartiles, which are not sensitive to outliers (small or large). The first quartile is the value that, when the data are sorted in ascending order, one-quarter (25%) of the data lies at or below this value, and three-quarters lie at or above it. The second quartile or median divides the data in half, and the third quartile lies at the value at which 75% of the data lies at or below this value. The three quartiles of the rain masses of the seeded and

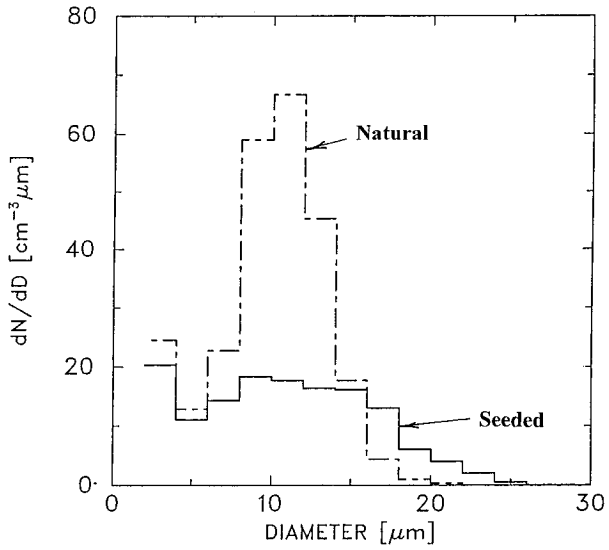

	Seeded	Natural
Time (SAST):	14:12:42	14:12:55
Liquid Water (g/kg):	0.33	0.35
Concentrations (cm^{-3}):	280	508

FIG. 9. Droplet size distributions measured about 200 m above cloud base in a seeded cloud. The dashed curve shows an example of the typical size distribution observed in most of the cloud, and thought to be natural. The solid line distribution, measured in the same cloud, is believed to be in the seeded portion of the cloud. The Learjet remained in the seeded portion of this cloud for a total of 3 s.

control storms in 10-min time windows from decision time ($t = 0$) are plotted in Fig. 11. Zero values of rain mass are included in these analyses.

Table 3 shows the one-tailed p values calculated using permutation tests testing the null hypothesis against the one-sided alternative, which states that the mean of the seeded storms is larger than the mean of the controls. Also listed in this table are the number of storms in each time interval with nonzero and zero rain masses and storms that have been tagged as missing. These are storms that have yet to be picked up by the tracking software and assigned a track number or storms that are dropped by the tracking software for various reasons such as mergers and splits or moving too close or too far away from the radar. Missing storms are not included in the quartile analyses. The 90% confidence limits for the differences between the quartiles (seeded minus controls) in kilotons are listed. These confidence intervals are also based on permutation tests for the difference between the quartiles. Confidence intervals with positive lower limits—that is, confidence intervals that *exclude* zero rain mass—indicate that the seeded storms have significantly larger quartiles than the control storms. This analysis indicates that the smaller storms (first quartile) are apparently responding to treatment first; the second quartile next, perhaps 20 min later; and the larger storms in the third quartile, last. Intuitively, this is a physically realistic result, since the length of the cycle from release of the seeding material at cloud base to its effect on precipitation growth aloft to rainfall on the ground should be roughly proportional to storm size. The three quartiles are plotted against a common rain mass axis, which shows that most of the radar-

TABLE 2. Seeding instruction strategy employed to make sure that the radar operator and cloud physics sampling pilots were ''blind'' as to treatment (seed or no seed).

Radar	Seeding aircraft	Action
Seed	No	No seed
Seed	Yes	Seed
No seed	Yes	No seed
No seed	No	Seed

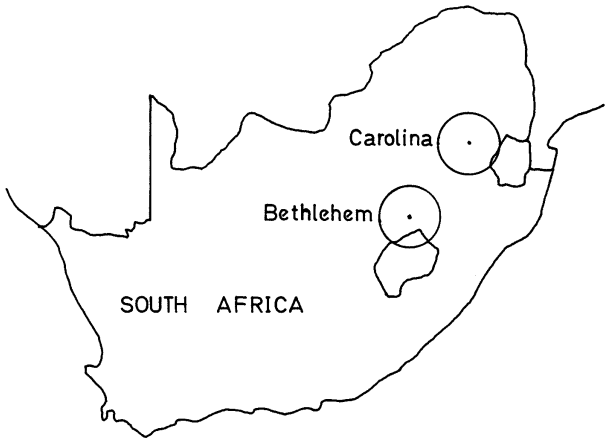

FIG. 10. The location of the two research areas in South Africa. The circles are centered around each radar and are 200 km in diameter.

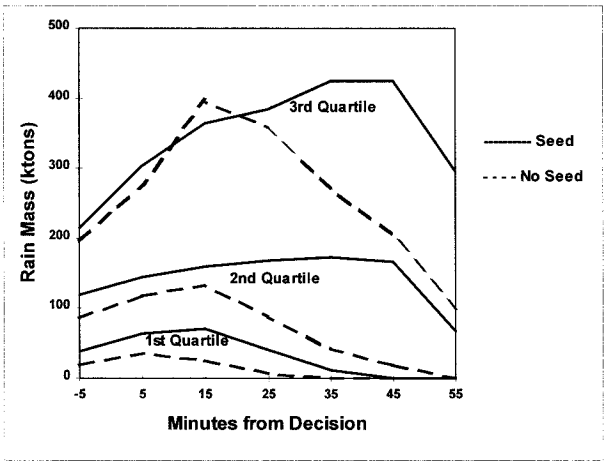

FIG. 11. Comparisons of the first, second, and third quartiles of the seeded vs the control group of storms. Note that the seeded storms peak later and at higher rain masses than their unseeded counterparts.

TABLE 3. Numbers of seeded and control storms in 10-min time windows either side of decision time and the *p* values for the differences (seeded minus control) of the three quartiles. The *p* values of 0.10 or less are in bold. The number of storms that are missing and have zero rain mass and the 90% confidence limits for the differences (kton) are shown in parentheses.

Time window (min)	Number of storms						One-tailed *p* values		
	Seeded			Control					
	(>0)	(Msg)	(0)	(>0)	(Msg)	(0)	Q_1	Q_2	Q_3
−10 to 0	60	(1)	(1)	59	(1)	(5)	0.22 (−8; 41)	0.20 (−38; 69)	0.34 (−60; 102)
0 to 10	61	(0)	(1)	60	(1)	(4)	0.16 (−8; 62)	0.28 (−38; 76)	0.25 (−93; 166)
10 to 20	60	(0)	(2)	56	(2)	(7)	**0.06** (3; 69)	0.23 (−32; 116)	0.57 (−146; 166)
20 to 30	56	(1)	(5)	50	(2)	(13)	**0.03** (6; 47)	0.14 (−34; 145)	0.40 (−114; 239)
30 to 40	48	(1)	(13)	44	(2)	(19)	**0.02** (4; 17)	**0.03** (34; 178)	**0.10** (−59; 338)
40 to 50	42	(2)	(18)	34	(3)	(28)	— —	**0.01** (34; 179)	**0.006** (72; 412)
50 to 60	37	(4)	(21)	25	(5)	(35)	— —	**0.03** (24; 87)	**0.02** (28; 385)

measured rainfall increases are coming from the medium to large storms. Since most of the seeding occurred in the first 20 min after decision time, the large third quartile difference between the seeded and control storms after about 35 min suggests that the hygroscopic seeding is affecting the dynamics of the storms. Invoking a dynamic effect at this stage must remain hypothetical, since we have no physical measurements that support such an effect.

c. Results—Exploratory analysis

Having established that seeding had a significant positive effect on the rain mass of storms (which was the prime objective), exploratory analyses of other storm properties follow. The dataset collected during the experiment is a very rich and interesting one, and the main purpose of the following analyses is to learn more about the behavior of storms responding to seeding.

The questions asked in this after-the-fact exploratory analysis are the following:

- Can any radar-measured differences between the seeded and control storms be sharpened by eliminating the larger storms from the data?
- Are these differences congruent with the hygroscopic seeding hypothesis and occurring in a physically plausible sequence?
- Can we develop from any of these differences a useful ''seeding signature'' algorithm? A reliable (low false alarm rate) radar-measured seeding signature would allow us to recognize in almost real-time storms that are responding to treatment.

The large storms were rejected by limiting the analysis to those storms whose volumes at decision time did not exceed 750 km^3, which reduced the number of storms from 127 to 96 (44 seeded, 52 controls). This partition was also used in the Nelspruit dry ice seeding experiment (Mather et al. 1996). It effectively eliminates squall lines and very large storms in which the seeded (or control) cell might be just one of many, all tracked as a single entity by the software.

It should be emphasized here that this after-the-fact exploratory analysis is not being used to attempt to demonstrate increases in rainfall from seeded storms. Clearly, some of the radar-measured response variables in this section are highly correlated (are measuring highly related storm properties). This is not a worry here—what would be of consequence would be the appearance of ''rogue'' track properties that are completely at odds with the others that appear in the 10-min time windows shown in Table 4. Thus, *p* values are used to measure the strength of the seed–no seed differences and not as measures of statistical significance. Here, two-tailed *p* values determined using standard permutation procedures are quoted since, in this exploratory analysis, we are not testing a one-sided hypothesis.

Those storm track properties that have *p* values equal to or less than 0.05 in 10-min time windows from decision time are listed in Table 4. Using this measure, the only track property that showed a difference between seeded and control storms in the 10-min time interval after decision time was the height of the maximum reflectivity, which exceeded the height of the reflectivity-weighted centroid (RWC). This response, heightened reflectivity aloft shortly after seeding commences, is an observation that is often noted by radar operators controlling the experiments (see Fig. 4). The next time window showed differences in maximum rates of increase in mean heights of storm tops, storm mass above 6 km, vertical centroids (centers of gravity), the heights of the 45-dB*Z* contours, the mean storm masses, and reflectivities as a function of height, all of which signal an increase in the top heaviness of the treated storms, a

TABLE 4. Storm track property differences whose seeded means were larger than the control storm means at p values of 0.05 or less in 10-min time windows from decision time.

0 to 10 min	10 to 20 min	20 to 30 min	30 to 40 min
Height (Max dBZ − Z_{wtd} centroid)	Maximum rates of increase in:	Maximum rates of increase in:	Storm duration
	echo top	—	max area @ 1.5°
	storm mass above 6 km	—	area–time integral
	vertical centroid	—	max rain flux @ 1.5°
	height of 45 dBZ contour	height of 45 dBZ contour	rain mass
	mass = f(Height)	—	max rain flux @ 6 km
	dBZ = f(Height)	—	max height 45 dBZ
	% volume = f(dBZ)	% volume = f(dBZ)	Maximum rates of increase in:
	storm area @ 1.5°	—	storm area @ 1.5°
		peak dBZ	—
	mean dBZ	mean dBZ	—
	—	rain flux @ 1.5°	rain flux @ 1.5°
	—	—	rain flux @ 6 km
	—	—	% area = f(dBZ)

Note: Rain flux ($m^3\ s^{-1}$) is the radar-measured rain rate ($m\ s^{-1}$) over a defined area (m^2); rain mass is the rain flux integrated over time(s).

measurement that is consistent with enhanced coalescence aloft. Also appearing are maximum rates of increase in storm area at lowest scan, mean reflectivity, and percent storm volume as a function of reflectivity. This latter track property indicates increases in the storm volume filled with higher reflectivities, that is, the seeded storms are becoming more dense. In the 20–30-min time period, the first appearance of an effect on rain measured at the lowest scan level appeared—differences in maximum rates of increase in rain flux between the seeded and control storms. Differences in maximum rates of increase in peak and mean reflectivities also occurred along with percent storm volume as a function of reflectivity. By 30 to 40 min after decision time, the differences in average storm duration, maximum area at 1.5°, the area–time integral, maximum rain flux at 1.5° and at 6 km, rain mass, and maximum heights of the 45-dBZ contour between the seeded and control storms all had p values of less than 0.05. Differences in maximum rates of increase at the lowest scan level in storm area, rain flux at 1.5° and 6 km, and percent storm area as a function of dBZ have also appeared. This last track property is similar to storm volume as a function of reflectivity. On average, higher reflectivities are increasingly filling a larger portion of the areas at the lowest scan level in the seeded storms, a response that we attribute to an increase in precipitation efficiency (more rainfall per unit storm area).

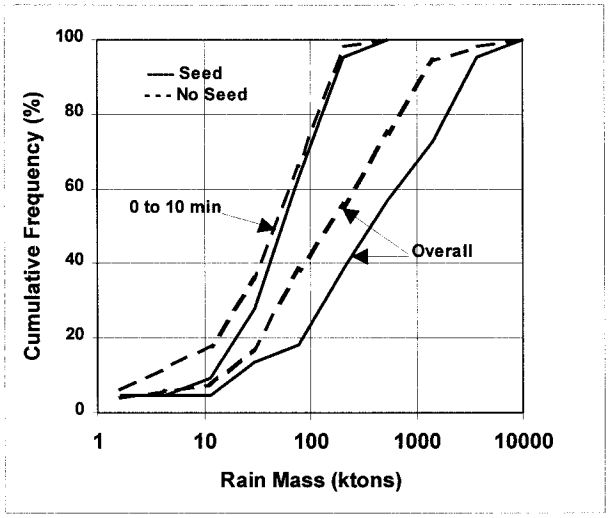

FIG. 12. Radar-measured rain masses accumulated in the 10-min time interval after decision time and from decision time onward in seeded and control storms whose volumes at decision time were equal to or less than 750 km^3.

Next, we look at overall storm track property differences from decision time onward. In this comparison, the seeded storms are lasting longer than the controls (p value of less that 0.01). This affects the time integrals of the average seeded storm volume, mass, area, and rain flux, which are all larger than the control averages at p values of less than 0.04. The comparison of seeded and control rain masses in the 0- to 10-min time interval to the accumulated rain masses over the lifetimes of the storms from decision time is shown in Fig. 12. The overall seeded distribution of rain mass differs from the control at a p value of 0.01.

The other track properties differences that score p values of 0.05 or less over the lifetimes of the storms after decision time are maximum rates of increase in cloud-top height, storm mass above 6 km, rain flux, RWC, mean dBZ, heights of the 45-dBZ contour and the peak dBZ, storm mass and reflectivity as a function of height, and percent storm volume as a function of reflectivity. Most of these differences are related to radar-detected increases in reflectivities aloft and increases in storm densities. The greater rate of increase in rain mass of seeded storms indicate that they are growing

TABLE 5. Radar-measured rain masses integrated over the 10 min following decision time and from decision time onward for those four classes of seeded and control storms whose peak reflectivities exceeded and remained below the RWC in the first 10 min after decision time.

Peak dBZ − RWC	Rain mass (ktons)			
	Seed		No seed	
	0 to 10 min	Overall	0 to 10 min	Overall
Positive	123	2358 (23)	119	509 (23)
Negative	129	1318 (21)	110	861 (29)

faster than the controls. Since larger storms appear to exhibit faster initial growth rates in rain mass (see Fig. 11), this result suggests that the seeding may be kicking smaller storms into larger categories by accelerating their growth rates.

What is important about this part of this exploratory analysis is that the time-resolved radar differences between seeded and control storms are commensurate with the hygroscopic seeding hypothesis. Higher reflectivities aloft are viewed as indications of enhanced coalescence in the treated storms (large drops) that, by harvesting more of the available supercooled water, produce more radar-measured rain at the lowest scan level. In addition, the time evolution of the storm track property differences follow each other at physically realistic intervals.

The heights of the maximum reflectivities in the first 10 min after decision time have a bimodal structure: one peak below the RWC, the other above. We now ask the question that leads to the last partition of the data in this exploratory analysis: Do the seeded storms that exhibit these elevated peak reflectivities in the first 10 min after decision time do any better than the others? The rain mass is divided into four groups: those whose peak reflectivities (seeded and control) exceed the RWC in the first 10 min after decision time (seed—23, control—23) and those whose peak reflectivities remain below the RWC (seed—21, control—29). The radar-measured accumulated rain masses in these four categories in the 10 min following decision time and from decision time onward are listed in Table 5.

The four rain masses are similar in the first 10 min after decision time, indicating an absence of inadvertent selection biases. Over their lifetimes from decision time, those seeded storms whose initial peak reflectivites exceed the RWC do considerably better than the controls in the same category, and better than the seeded storms whose peak reflectivities do not exceed the RWC in the 10 min after decision time. Conversely, the control storms whose initial peak reflectivities exceed the RWC do not do as well as those with negative excursions. This result suggests that an initial positive excursion of a storm's peak reflectivity above the RWC, seen in real time with storm tracking software, may signal a successful seeding event. The implications of the ability to detect reliably a seeding response from treated storms are discussed in the conclusions section of this paper.

4. Discussion and conclusions

At this stage, our seeding hypothesis needs expanding. By enhancing coalescence by hygroscopic seeding at cloud base, more of the water ingested by the treated storms is turned around before it is expelled into the anvil. This results in an increase in the efficiency of the rainfall process (a greater portion of the water vapor is returned to the ground as precipitation). Turning more water around earlier implies greater loading of the updraft by the larger particles with a concomitant increase in the downdraft. It is this invigorated storm outflow that undercuts more of the warm air to trigger new and more vigorous cloud growth on the flanks of the treated storms.

The question of whether the seeding alters the drop spectra sufficiently to produce an apparent radar-measured increase in rain mass by just shifting the existing rain mass into fewer, but larger drops (narrow spectra) deserves mention. The seeding may alter the drop size distribution at high levels in the treated clouds, but by the time these drops fall to the levels scanned by radar for measuring rain mass, the drop-size distribution will have been readjusted by natural processes so that any differences between seeded and control storm rainfall drop spectra will no longer be detectable (Cunning 1976). Srivastava (1967) computed the evolution of raindrop size spectra by coalescence between raindrops and found that, while exponential distributions change slowly with time, narrow distributions develop rapidly into exponential distributions.

In any weather modification operations or experiments with convective clouds, situations will arise when seeding will not be effective. Such failures can be a result of the following:

- clouds that will not respond to treatment (cloud bases too high or too low),
- poor delivery techniques, and/or
- defective seeding material.

It will be a great step forward in the field of weather modification if we can learn to recognize, using radars, the characteristics of clouds that are responding to treatment, to separate the seeding successes from the failures, and further, to be able to assign likely reasons for the apparent failures thus exercising a sort of cloud-seeding quality control. The ability to take this step forward will depend on real-time storm-tracking routines (already available, see Dixon and Weiner 1993) and the development of a radar-measured seeding signal algorithm with a low false alarm rate. The work reported here in the exploratory experiment suggests that we may be close to realizing this goal. Such a development would also simplify the transferability of a successful convective cloud-seeding technology. The seeding methods

and materials could be tested for a response on the clouds in new regions before proceeding with the design of time-consuming randomized experiments.

This paper marks the conclusion of over 15 years of continuous research in South Africa into convective clouds and their response to various seeding materials. The long convective season in the research areas (about 6 months) provides an almost ideal laboratory for such research. Initially, experiments were conducted with silver iodide, using both droppable and end-burner flares. Since the aim was to grow large particles as fast as possible, the apparent slow build up of ice crystals in test clouds seeded with silver iodide led to experiments using dry ice. Here, measurements showed that massive amounts of ice were produced in a very short time and that the dispersion of the ice crystals so produced was superior to anything recorded using silver iodide flares.

The idea of a dynamic response to glaciogenic seeding in South African storms as the basis of our seeding hypothesis was soon abandoned. Most storms have sufficient buoyancy to reach the tropopause without any additional heat release from the early freezing of supercooled water (even if this could be achieved). Early on, our goal became the attempt to harvest more of the supercooled water in the strong updrafts before the small particles containing this water could be spilled into the high anvil clouds that are a characteristic of these storms. Dry ice appeared to be the best bet at the time, so a 3-yr randomized experiment was conducted. It was during the course of this experiment that the importance of coalescence as a precipitation formation mechanism began to be cautiously appreciated. (Recall that at this time, most experimental efforts in the Northern Hemisphere were concentrating on ice processes). The dry ice experiment showed positive results after the data were partitioned to include in the analysis only those clouds that stood a good chance of developing water drops via coalescence. So the seeding hypothesis that we embraced was an old one first suggested by Braham (1964) and later supported numerically by Johnson (1987), that frozen drops would grow faster as graupel than as liquid water drops. But this raised additional problems since observations showed that when coalescence was active, there appeared to be enough ice being generated by some sort of secondary ice multiplication process, so why add more?

The difficulty at this stage of the research was to conceptually and observationally link the massive amounts of ice that could be produced around $-10°C$ to more rainfall on the ground. It was at this juncture that serendipity played a part; our encounter with a large convective storm growing over a Kraft paper mill. The unique nature of this storm was only recognized against the extensive cloud physics database that we had acquired after some 10 years of sampling convective clouds with our instrumented Learjet. Here was a storm that was producing huge drops (4–6 mm in diameter) at $-10°C$ in a 15 m s^{-1} updraft! This encounter changed the direction of our research, for if such inadvertent modification could take place in a large convective storm, perhaps we could learn to achieve the same objective through planned intervention. The rest of the study is reported above.

Our assertion that rainfall can be augmented from large multicell storms by seeding at cloud base with hygroscopic flares is supported by cloud physics measurements, randomized experiments, and numerical calculations. Our seeding hypothesis is that by accelerating the coalescence processes in treated storms, more of the available supercooled water is harvested before being expelled into the anvil, thereby increasing the efficiency of the rainfall process. While not on as firm a base as the precipitation efficiency aspect of the hypothesis, we also believe there is evidence that increasing precipitation efficiency produces dynamic consequences, which lengthen storm lifetimes by strengthening storm outflow, which in turn leads to more vigorous new cell development on the flanks of treated storms.

Results of calculations and some model results suggest that in clouds with very maritime droplet spectra (100 droplets per cubic centimeter), hygroscopic seeding will have no effect on the rain process, since coalescence is already very efficient in such storms (Reisin et al. 1996).

The work with this new seeding technique is just beginning. It would be extremely fortuitous if the first hygroscopic seeding flare was ideal for all convective cloud-seeding applications. Much work needs to be done on optimizing the dry particle spectrum and perhaps the chemical composition of the flares. This will require sophisticated measurements coupled with numerical calculations. The dynamic aspects of the seeding hypothesis can possibly be tested using three-dimensional cloud models. Additionally, the apparent sensitivity of convective storms to relatively small changes in aerosol inputs raises questions about the impact of pollution from industrial sources, biomass burning, etc., on the efficiency of the precipitation processes of convective clouds growing in highly polluted atmospheres.

While we have shown that rainfall can be increased from individual storms, we have still to demonstrate that rainfall can be augmented over an area. This task, which is now being tackled on two fronts in South Africa by a research program in the Bethlehem area and an operational cloud-seeding program in the Northern Province, will attempt to demonstrate to water users that the new technology can have a positive impact upon the water resources of a region. The magnitude of this task should not be underestimated; it was at this stage that many previous rain augmentation efforts foundered.

Acknowledgments. The work reported here comes from the combined efforts of the personnel of the National Precipitation Research Program (NPRP), which is an amalgamation of the Weather Bureau team at Beth-

lehem, the staff of CloudQuest at Nelspruit, and the statistical team at Unisa.

Central to the success of this research has been the continuity in the research funding provided by the Weather Bureau and the WRC, the inspiration supplied by two chief directors of the Weather Bureau, Piet du Toit and Gert Schulze, and the unflagging support of Dr. George Green, the NPRP's project coordinator.

REFERENCES

Biswas, K. R., and A. S. Dennis, 1971: Formation of a rain shower by salt seeding. *J. Appl. Meteor.*, **10,** 780–784.

Braham, R. R., Jr., 1964: What is the role of ice in summer rain showers? *J. Atmos. Sci.*, **21,** 640–645.

Cooper, W. A., R. T. Bruintjes, and G. K. Mather, 1997: Some calculations pertaining to hygroscopic seeding with flares. *J. Appl. Meteor.*, **36,** 1449–1469.

Cunning, J. B., Jr., 1976: Comparison of the *Z–R* relationship for seeded and nonseeded Florida cumuli. *J. Appl. Meteor.*, **15,** 1121–1125.

Dennis, A. S., E. W. Holroyd III, W. E. Howell, D. A. Matthews, B. A. Silverman, and A. B. Super, 1984: HIPLEX: A co-operative program on rain augmentation in the High Plains. Bureau of Reclamation, Denver, CO, 55 pp. [Available from Water Research Commission, P.O. Box 824, Pretoria 001, South Africa.]

Dixon, M. J., and G. K. Mather, 1986: Program for atmospheric water supply—Phase I, 1983–86, Vol. III. WRC Rep. 133/3/88, Pretoria, South Africa, 55 pp. [Available from Water Research Commission, P. O. Box 824, Pretoria 001, South Africa.]

——, and G. Wiener, 1993: TITAN: Thunderstorm identification, tracking, analysis and nowcasting—A radar-based methodology. *J. Atmos. Oceanic Technol.*, **10,** 785–797.

Eagan, R. C., P. V. Hobbs, and L. F. Radke, 1974: Particle emissions for a large Kraft paper mill and their effects on the microstructure of warm clouds. *J. Appl. Meteor.*, **13,** 535–552.

Garstang, M., G. D. Emmitt, and B. Kelbe, 1981: Rain augmentation in Nelspruit (RAIN). Report to the WRC, Pretoria, South Africa, 266 pp. [Available from Water Research Commission, P.O. Box 824, Pretoria 001, South Africa.]

Hindman, E. E., 1978: Water droplet fogs formed from pyrotechnically generated condensation nuclei. *J. Wea. Modif.*, **10,** 77–96.

Johnson, D. B., 1987: On the relative efficiency of coalescence and riming. *J. Atmos. Sci.*, **44,** 1671–1680.

Klazura, G. E., and C. J. Todd, 1978: A model of hygroscopic seeding in cumulus clouds. *J Appl. Meteor.*, **17,** 1758–1768.

Marshall, J. S., and W. M. K. Palmer, 1948: The distribution of rain drops with size. *J. Meteor.*, **5,** 165–166.

Mather, G. K., 1991: Coalescence enhancement in large multicell storms caused by the emissions from a Kraft paper mill. *J. Appl. Meteor.*, **30,** 1134–1146.

——, M. J. Dixon, and J. M. de Jager, 1996: Assessing the potential for rain augmentation—The Nelspruit randomised convective cloud seeding experiment. *J. Appl. Meteor.*, **35,** 1465–1482.

Morgan, G., B. J. Morrison, and G. K. Mather, 1989: Measurement of total and condensed water mixing ratios in warm based cumulus clouds by a jet engine evaporation technique. *Theor. Appl. Climatol.*, **40,** 187–199.

Reisin, T., S. Tzivion, and Z. Levin, 1996: Seeding convective clouds with ice nuclei or hygroscopic particles: A numerical study using a model with detailed microphysics. *J. Appl. Meteor.*, **35,** 1416–1434.

Srivastava, R. C., 1967: On the role of coalescence between rain drops in shaping their size distributions. *J. Atmos. Sci.*, **24,** 287–292.